

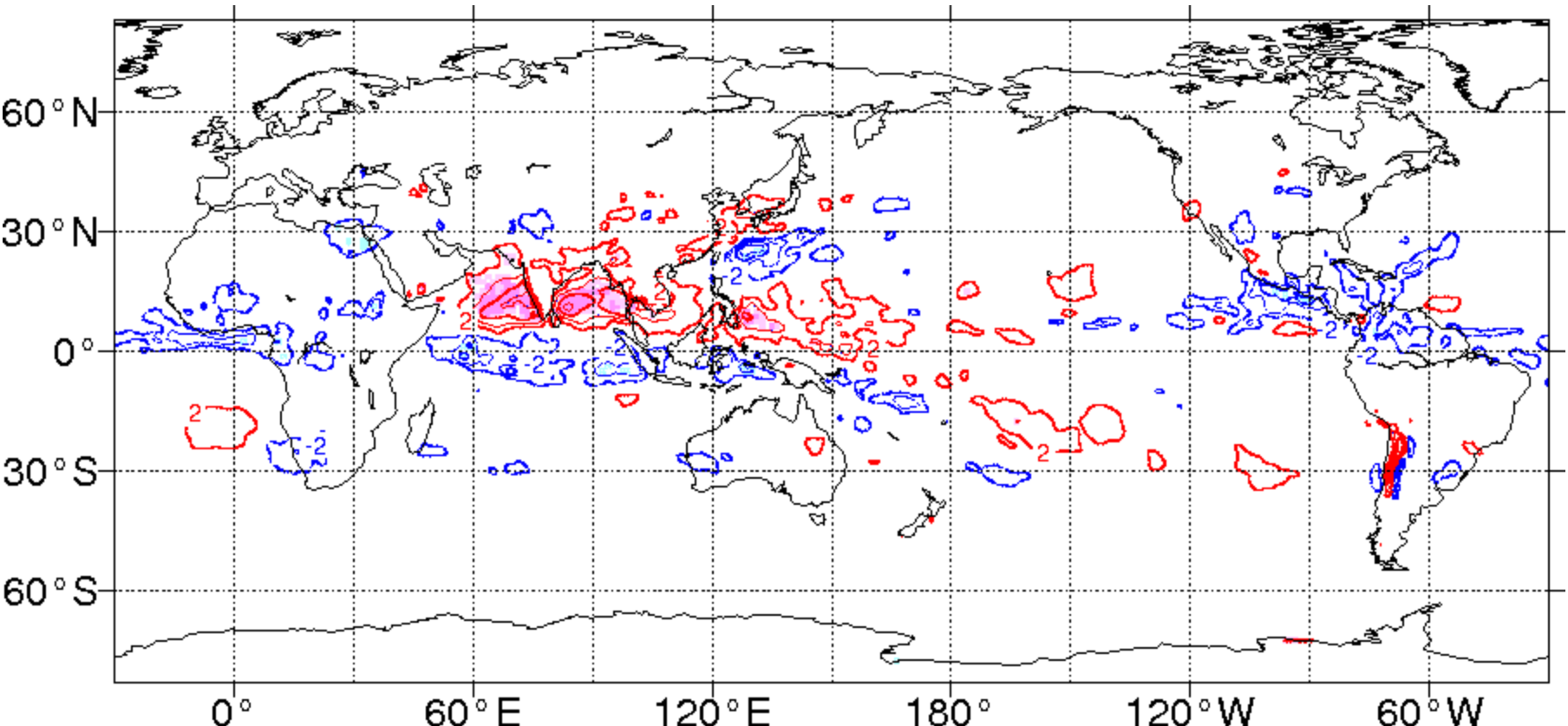
北半球夏季季節内振動明瞭時における 大気大循環場の特徴

原田やよい(気象研究所)

2018年9月4日(火)
波と平均流の相互作用に関する研究会 第6回打ち合わせ

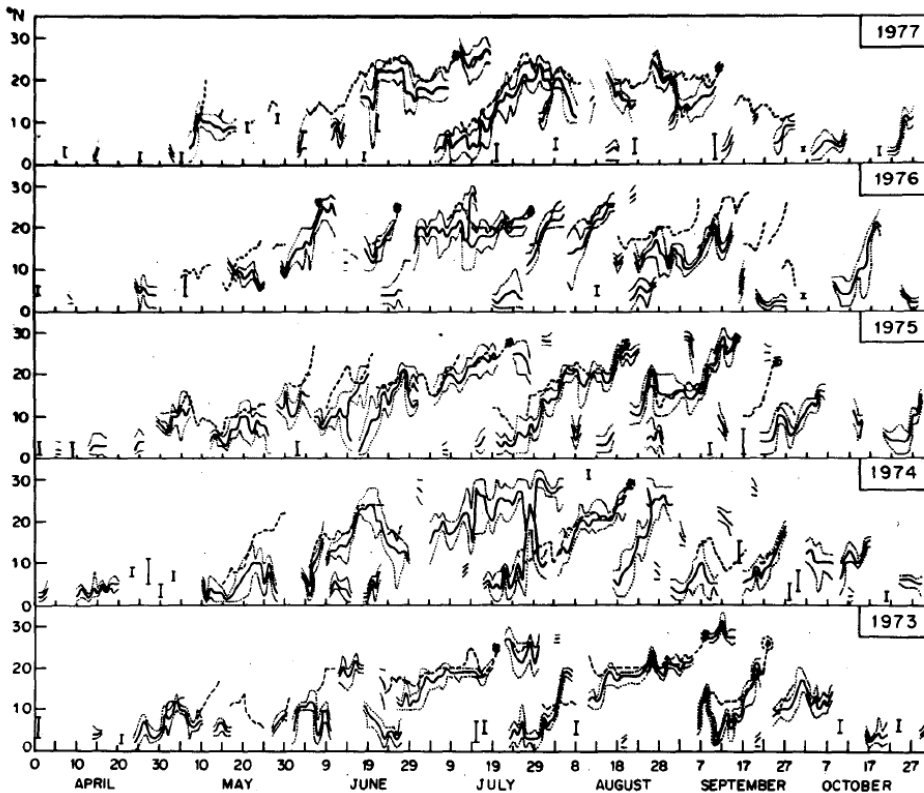
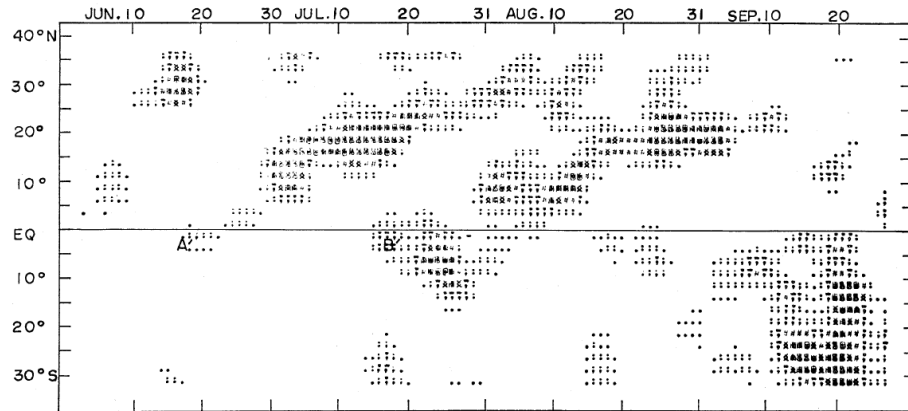
Introduction of BSISO#1

- Boreal Summer ISO (BSISO)... the dominant mode in boreal summer and active convective region migrates northward in the Indian Ocean and in the western Pacific Ocean



Example of life cycle of BSISO mode. Vertical velocity anomalies (contours of $4 \times 10^{-2} \text{ Pa s}^{-1}$) on 340 K surface.

Introduction of BSISO#2



- Yasunari 1979:

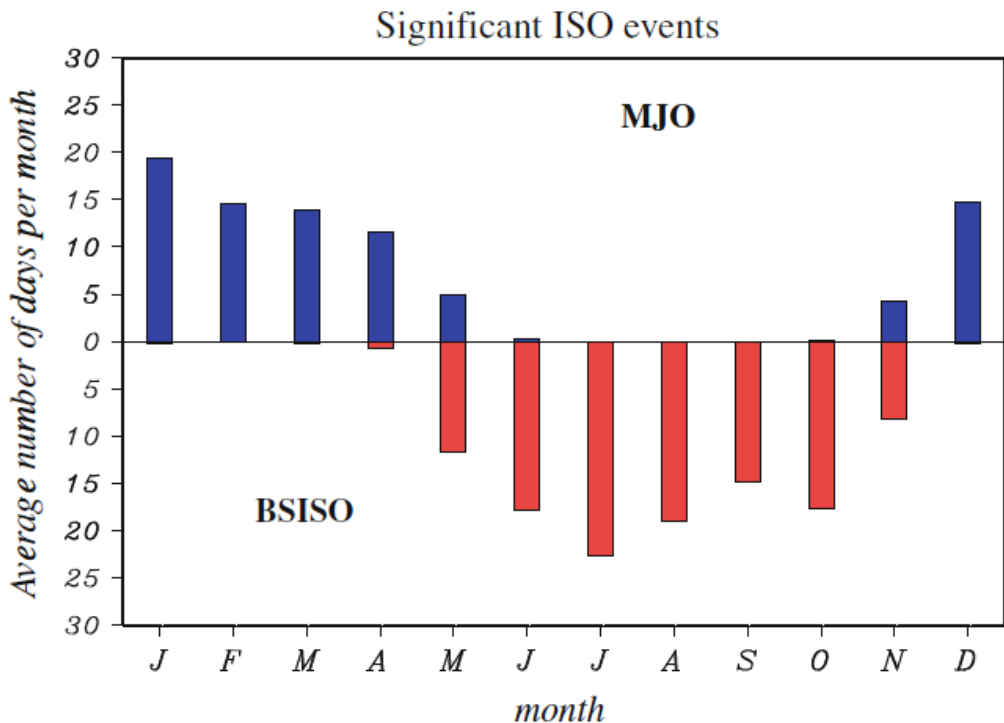
The broad-scale fluctuations of cloudiness over the Eastern Hemisphere during the northern summer monsoon were investigated by using daily satellite mosaic pictures. It is suggested that the fluctuation of 40-day period may be closely connected with the global-scale zonal oscillation in the equatorial zone and that of 15-day period may exist as a result of meridional wave interactions.

- Sikka and Gadgil 1980:

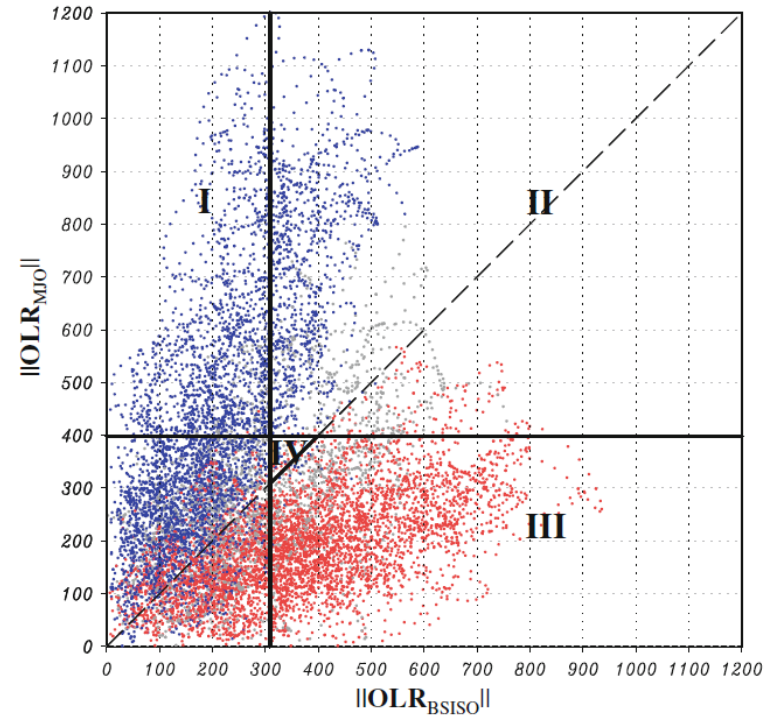
They extended the investigation period to 1973-1977.

Introduction of BSISO#3

MJO amplitude versus BSISO amplitude

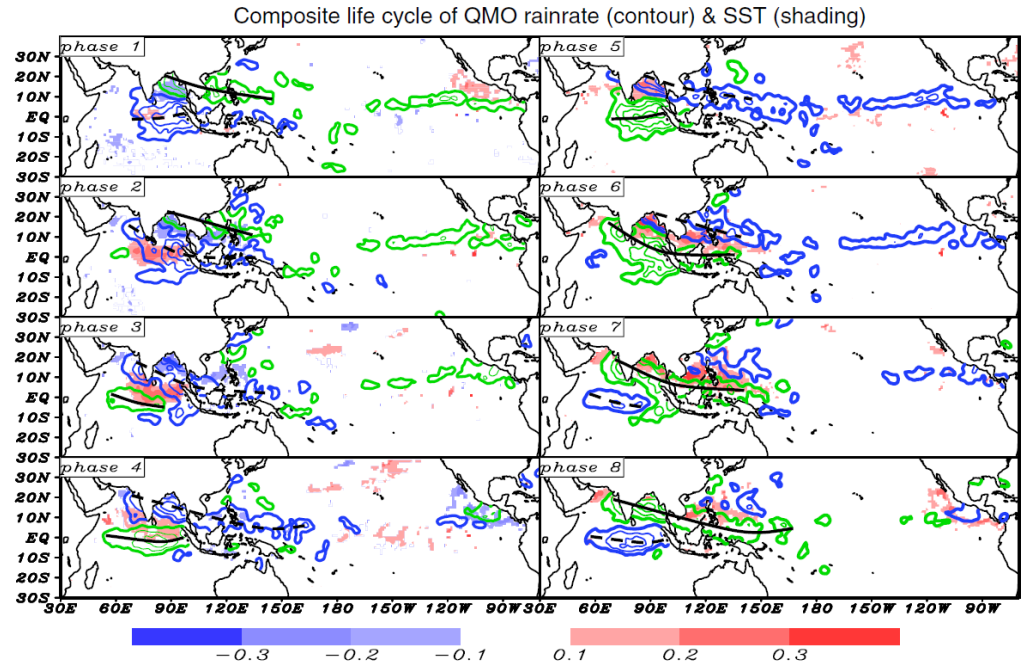


Average number of days during which significant ISO is present in a month



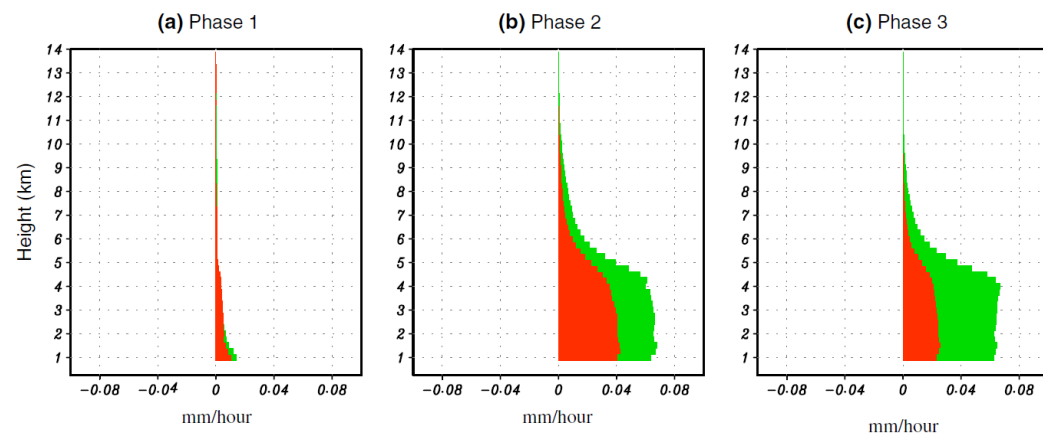
Scatter plot of ISO amplitude in terms of the BSISO mode (x axis) and the MJO mode (y axis) for the period 1979–2009.

Introduction of BSISO#4



► Wang et al. 2006:

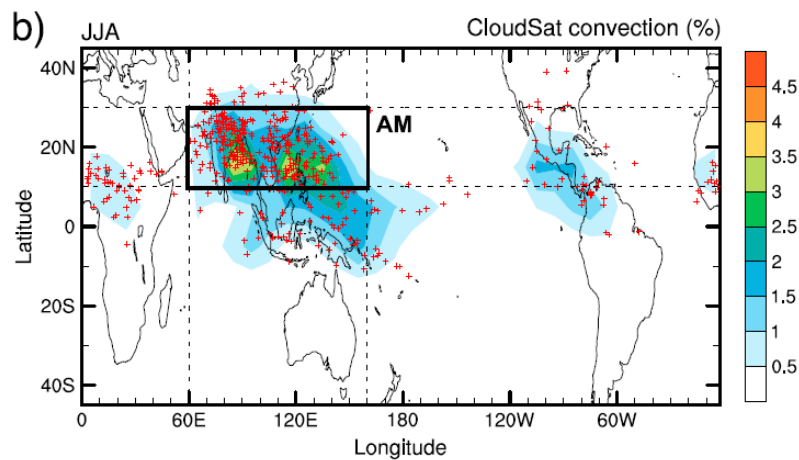
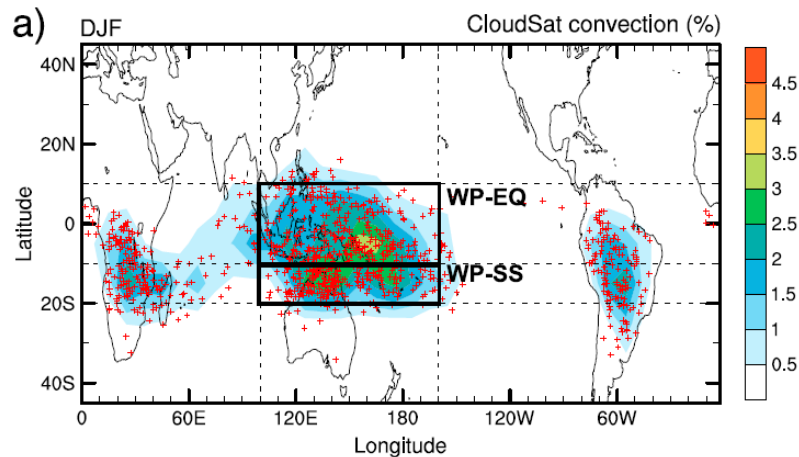
A composite scenario was made of 28 selected events with reference to the oscillation in the eastern equatorial Indian Ocean (EIO), where the oscillation is most regular and its intensity is indicative of the strength of the subsequent northward propagation.



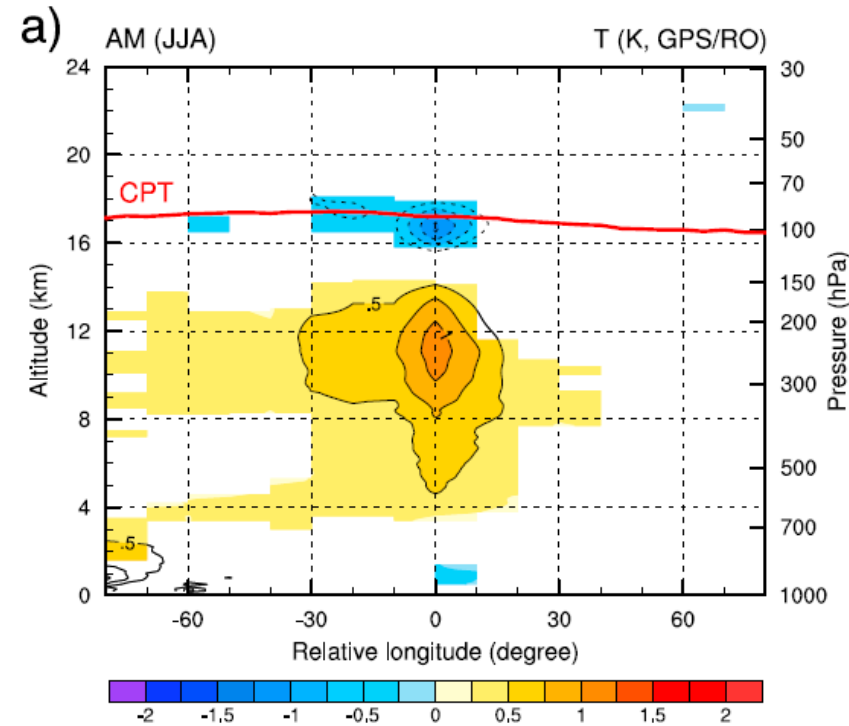
During the initiation of the convective anomalies, the stratiform and convective rains have comparable rates; the prevailing cloud type experiences a tri-modal evolution from shallow to deep convection, and finally to anvil and extended stratiform clouds.

The tropical convection in the B. S. season (JJA)

Kim et al. 2018



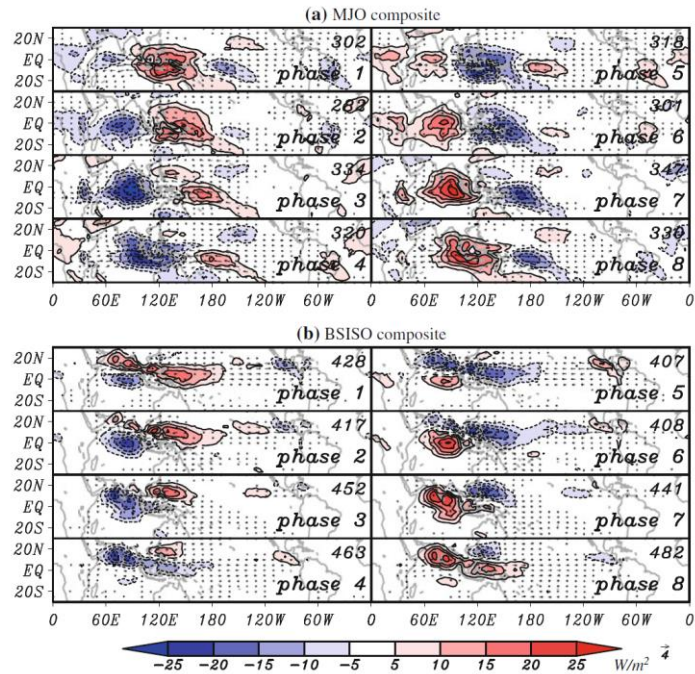
Spatial distribution of the tropical convection observed by CloudSat. Frequency distribution of deep convection higher than 15 km is shown as shading (%), and extreme cases (cloud top height > 17 km).



Composited temperature anomalies for extreme convection (cloud top height > 17 km) over AM in JJA. Contour intervals are 0.25 K (0, ± 0.25 contours are omitted) for upper panel, and 0.5 K for lower panel.

Data and Methods #1

- ▶ BSISO indices (Kikuchi et al. 2012)
 - ▶ Application of the extended EOF analysis to 25-90 band-pass filtered OLR
 - ▶ Projection of the time filtered OLR onto both MJO and BSISO modes
- ▶ JRA-55 reanalysis (Kobayashi et al. 2015)
 - ▶ model analysis fields for MIM method, isentropic analysis fields for map composites
 - ▶ Analysis period: 1979-2017 May - September
- ▶ Three-dimensional (3D) structure of mass-weighted isentropic time-mean (T-MIM) (Kanno and Iwasaki 2018)
- ▶ Lanczos filter (Duchon 1979)
 - ▶ 25-90 day band pass filter, 90,180-day low pass filter are applied
 - ▶ No filtered data is also used for composite analysis



Composite life cycle of (a) the MJO mode and (b) the BSISO mode. OLR anomalies (shades and contours of $5 Wm^{-2}$) and 850 hPa horizontal winds (vectors).

Figure 8 in Kikuchi et al. 2012

Data and Methods #2

Kanno and Iwasaki (2018)に基づきT-MIM法をJRA-55気圧面プロダクトに適用。

$$\sigma(x, y, \theta, t) \equiv -\frac{1}{g} \frac{\partial p}{\partial \theta},$$

$$\overline{A^*}(x, y, \theta) \equiv \frac{\overline{\sigma A}}{\overline{\sigma}}.$$

$$A'(x, y, \theta, t) \equiv A - \overline{A^*}.$$

単位温位当たりの質量
&

質量加重付時間平均(ここでは31日平均)
&

T-MIMからの偏差(短周期擾乱)

(7)

Stationary component: 31-day mass-weighted isentropic time mean

Transient component: deviation from 31-day

定常波成分と短周期擾乱成分に
分離可能

$$\begin{aligned}\overline{(AB)^*} &= \overline{\frac{\sigma AB}{\sigma}} = \overline{\frac{\sigma(\overline{A^*} + A')(\overline{B^*} + B')}{\sigma}} \\ &= \overline{A^*} \overline{B^*} + \overline{(A'B')^*},\end{aligned}$$

where $\overline{(\sigma A')} = 0$ and $\overline{(\sigma B')} = 0$ are used to derive right-hand side.

東西風の運動方程式を v^* について整理すると、東西風の時間変化項、移流項、3D EP fluxの収束・発散、外部強制の総和として表現できる。

$$\overline{v^*} = \frac{1}{f} \left(\frac{\partial \overline{u^*}}{\partial t} + \overline{\mathbf{v}^*} \cdot \nabla \overline{u^*} + \dot{\theta}^* \frac{\partial \overline{u^*}}{\partial \theta} \right) - \frac{1}{f \overline{\sigma}} \nabla \cdot \overline{\mathbf{F}} - \frac{1}{f} \overline{X^*}. \quad (22)$$

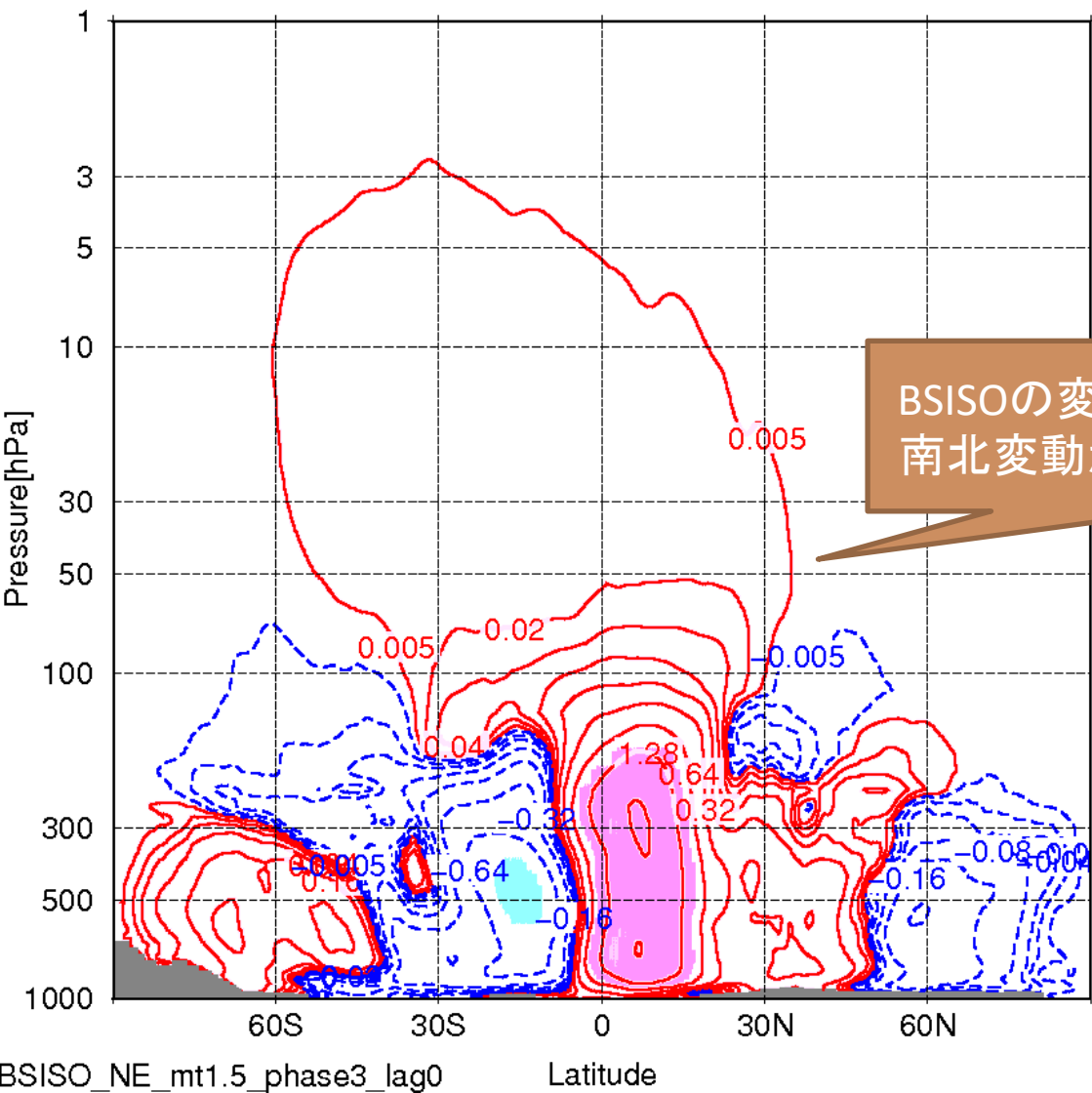
$$\nabla \cdot \overline{\mathbf{F}} \equiv -\nabla \cdot \left[\overline{\sigma(u'v')^*} \right] - \frac{\partial}{\partial \theta} \left[\overline{\sigma(u'\theta')^*} \right] - \overline{\sigma \left(\frac{\partial M}{\partial x} \right)_\theta}. \quad (23)$$

BSISOと（対流圏）大気大循環場との関係

Impact of BSISO on the Hadley and B.D. circulations

amplitude ≥ 1.5 SD, Day 0 to Day +20 for the phase 3

ENSO neutral condition,



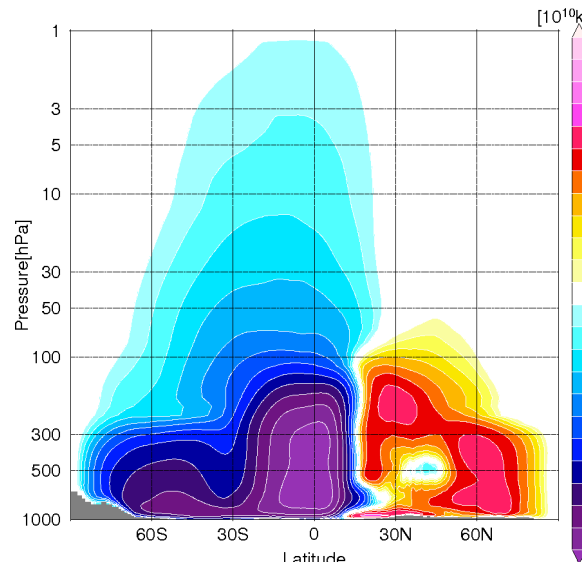
Light (dark) shadings show statistical significance at 90 % (95 %) confidence levels.



95 days
19 ESS (Effective Sample Size)

Summer (JJA) mean climatology

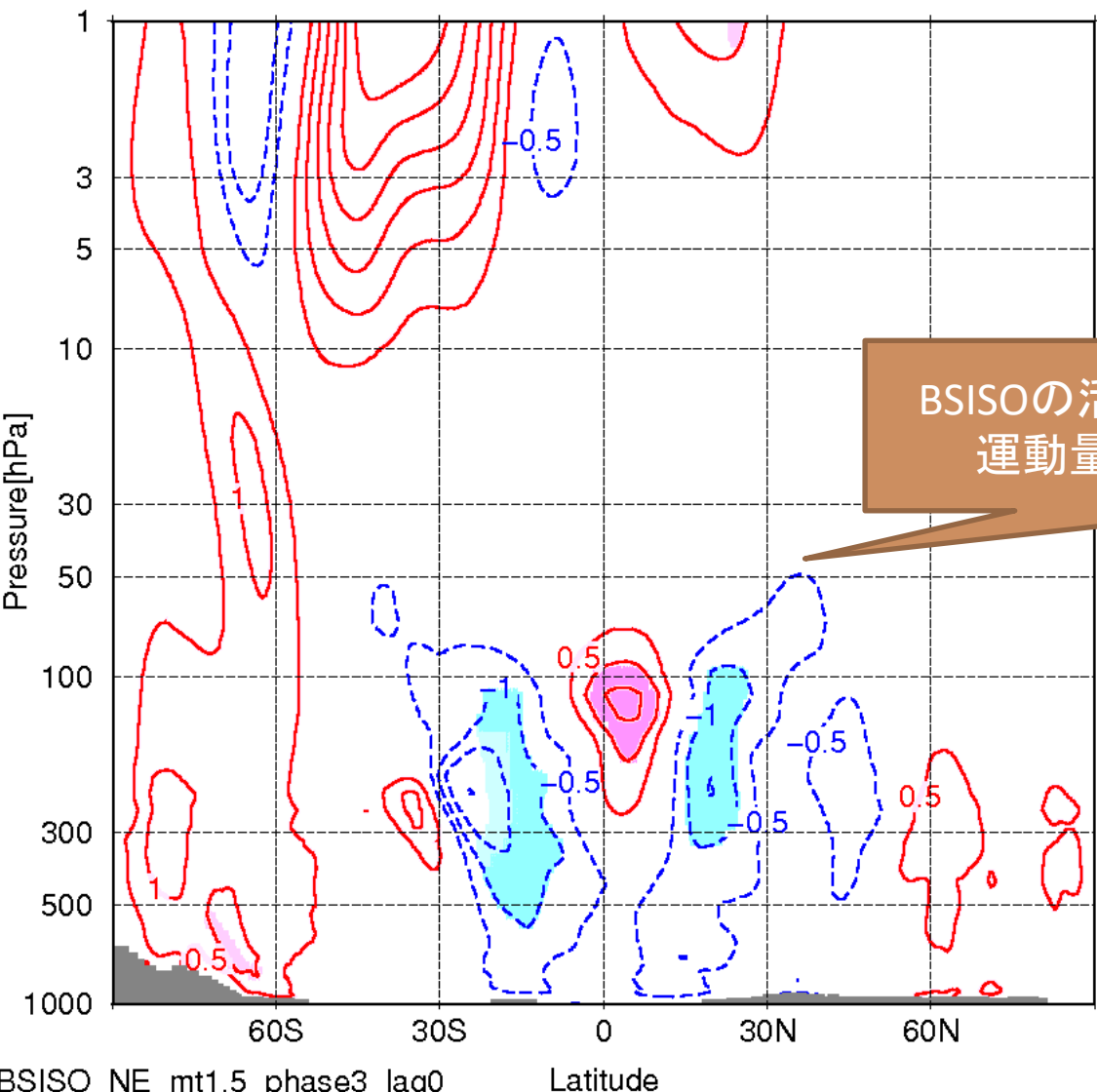
Mass stream function [$\times 10^{10} \text{ kg s}^{-1}$]



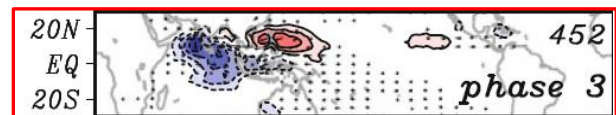
Impact of BSISO on the tropospheric zonal wind fields

amplitude ≥ 1.5 SD, Day 0 to Day +20 for the phase 3

ENSO neutral condition,



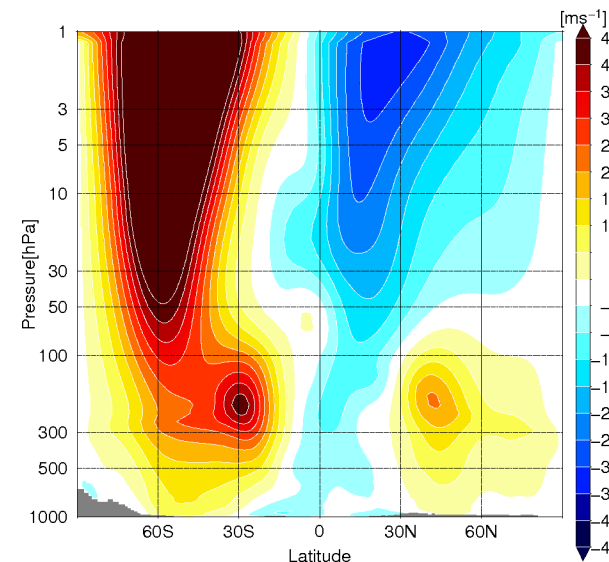
Light (dark) shadings show statistical significance
at 90 % (95 %) confidence levels.



95 days
19 ESS (Effective Sample Size)

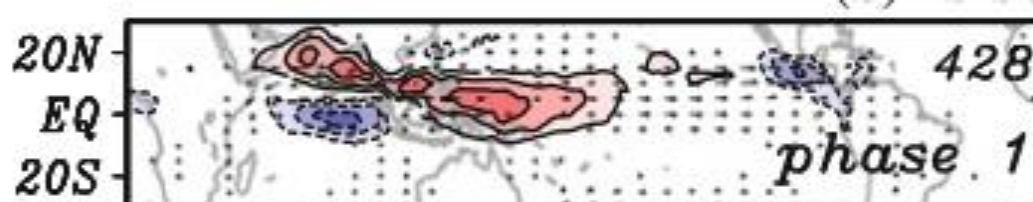
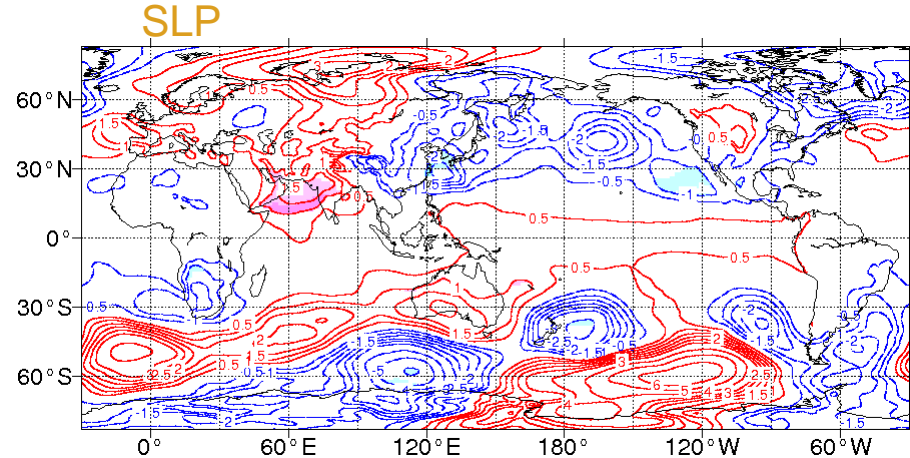
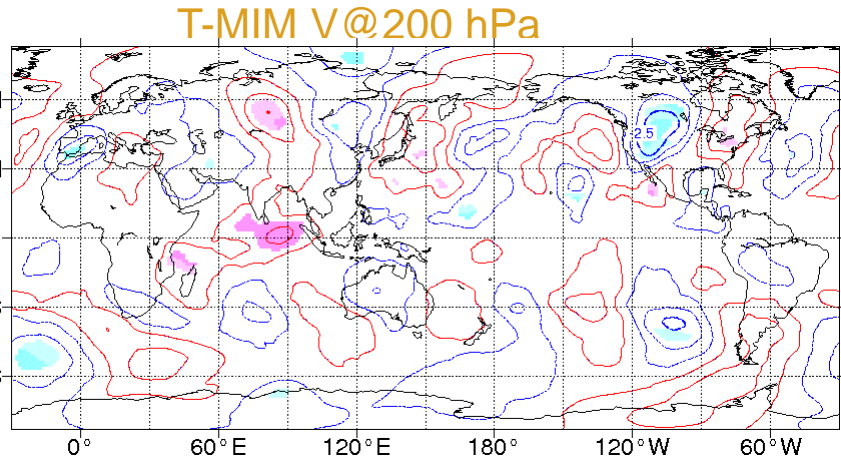
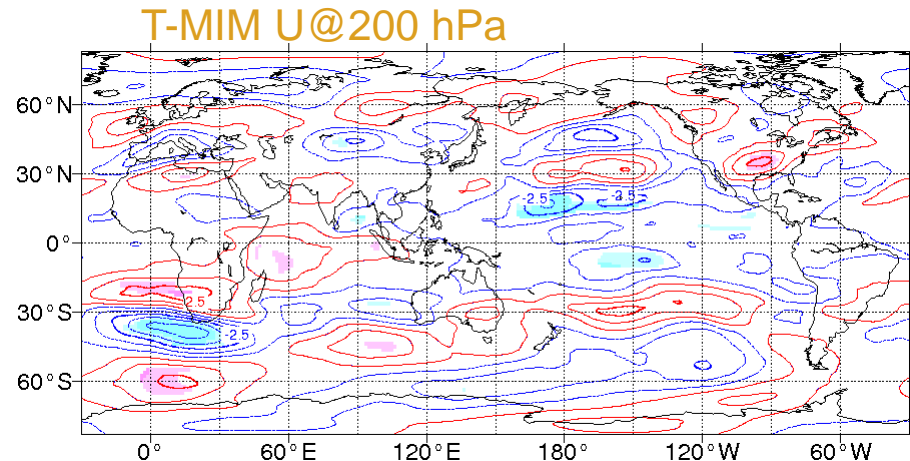
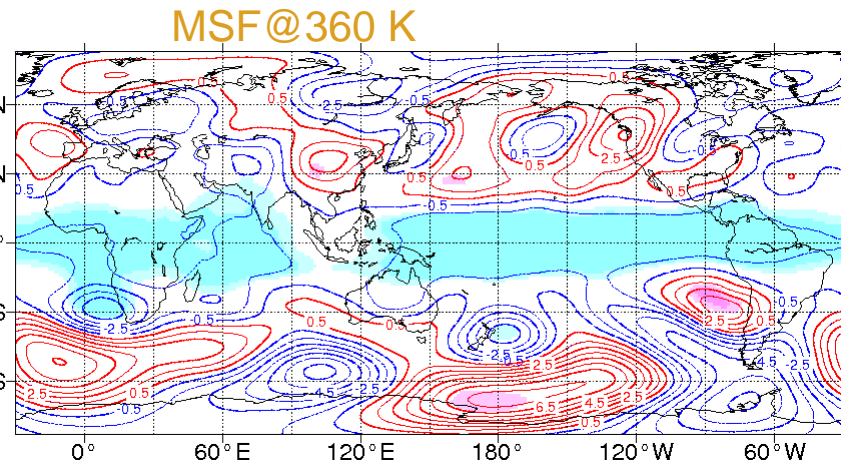
BSISOの活発位相の北進後、低緯度帯で運動量の極向きへの輸送が明瞭。

Summer (JJA) mean climatology
Zonal wind [$m s^{-1}$]



Features of the global atmosphere during remarkable BSISO amplitude ≥ 1.5 SD for the ENSO neutral condition

Phase1

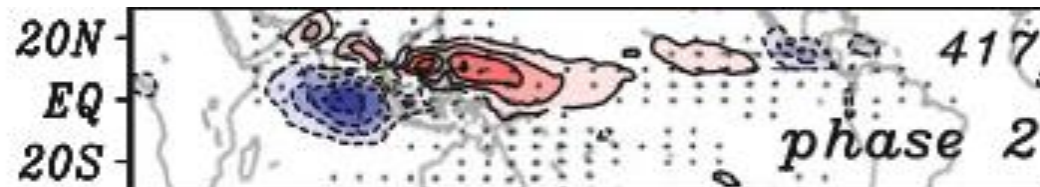
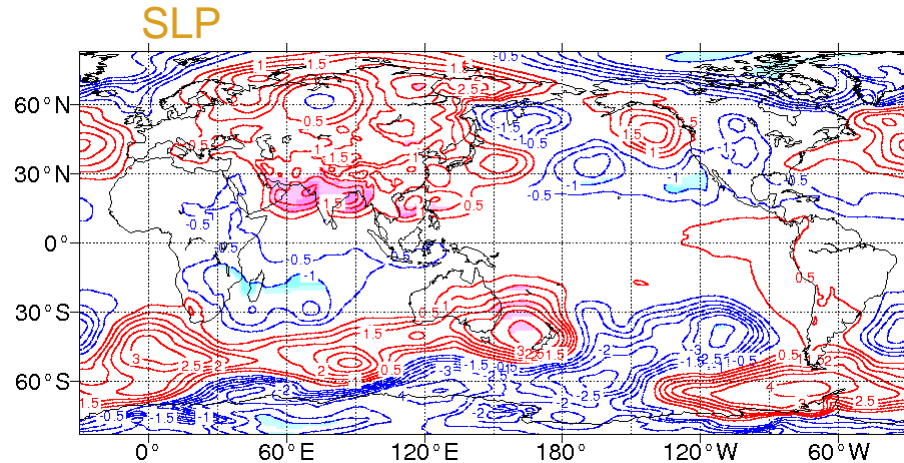
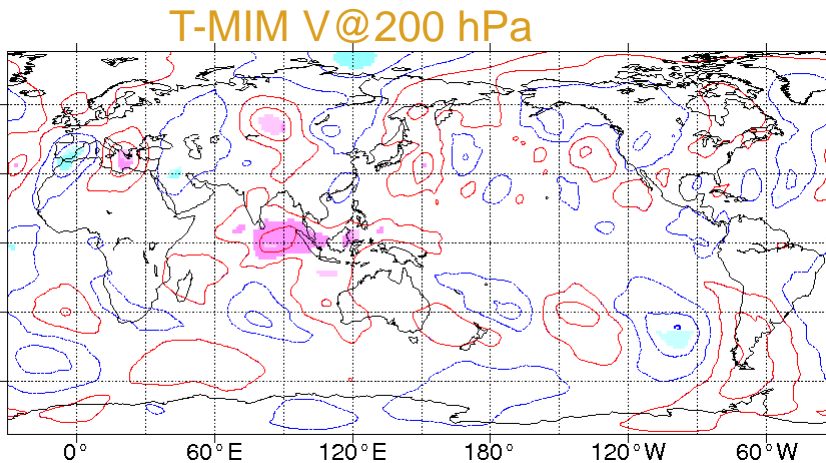
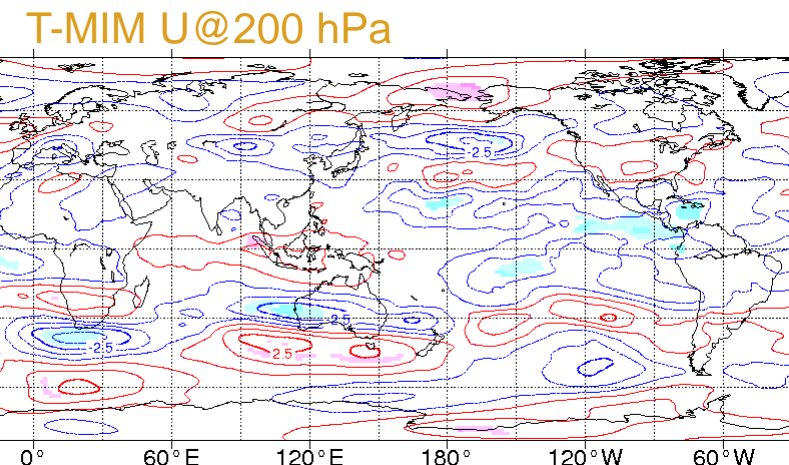
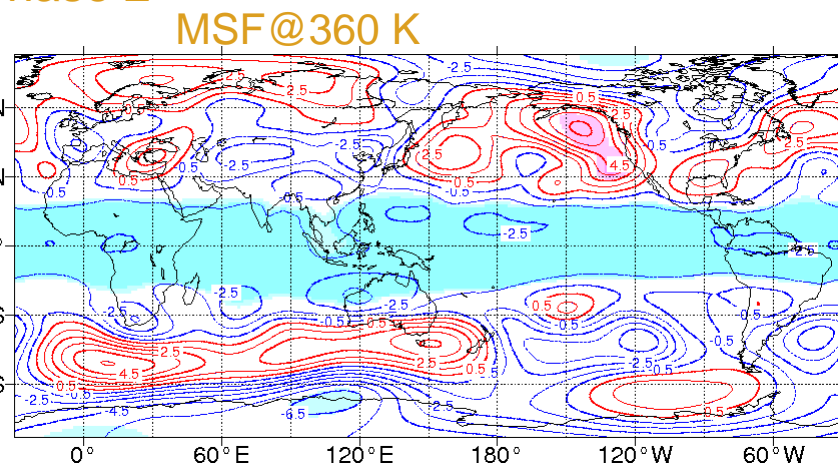


117 days
25 ESS
(Effective Sample Size)

Light (dark) shadings show statistical significance at 90 % (95 %) confidence levels.

Features of the global atmosphere during remarkable BSISO amplitude ≥ 1.5 SD for the ENSO neutral condition

Phase 2

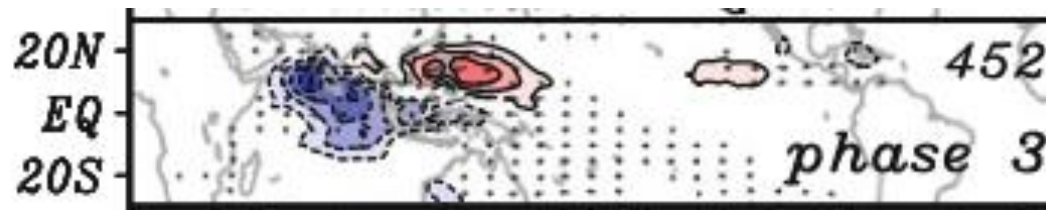
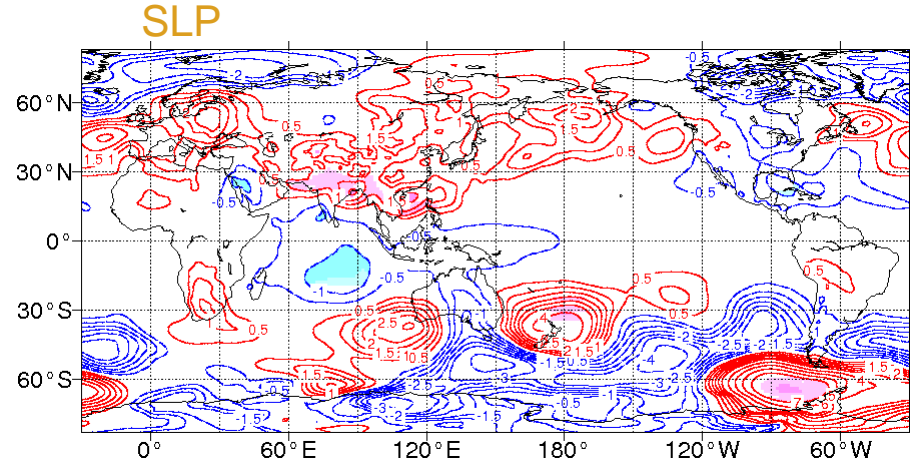
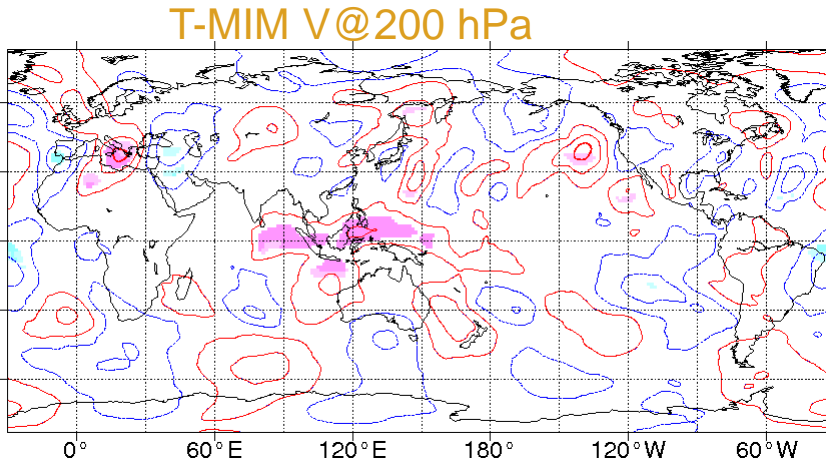
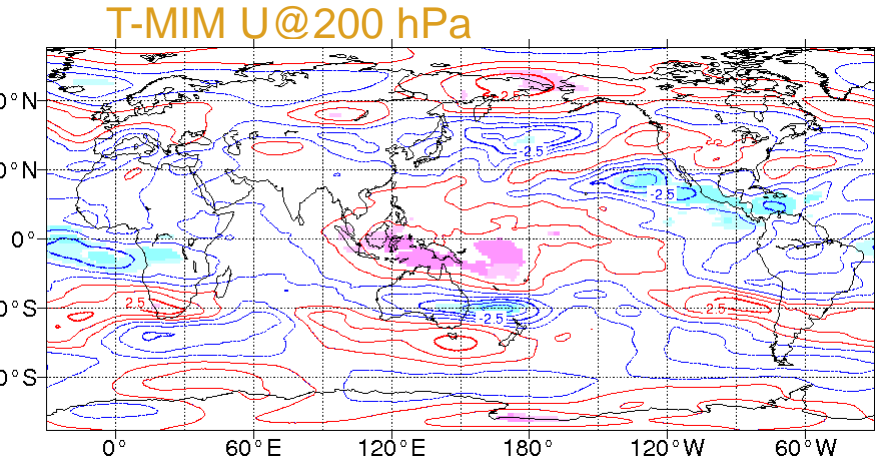
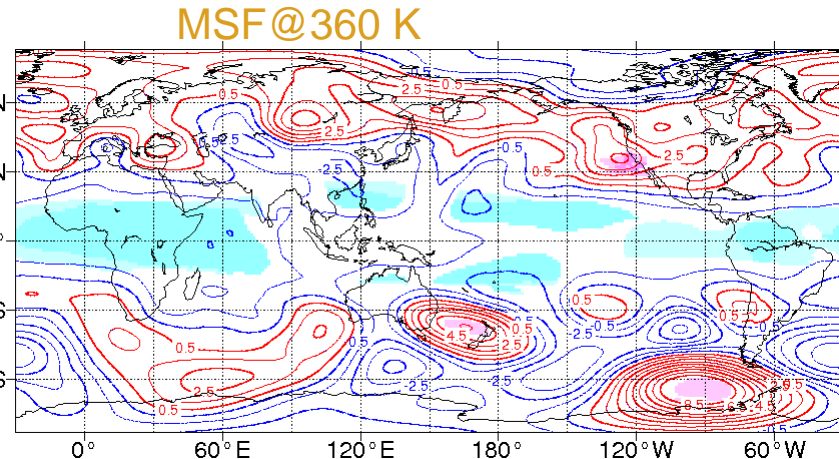


96 days
23 ESS
(Effective Sample Size)

Light (dark) shadings show statistical significance at 90 % (95 %) confidence levels.

Features of the global atmosphere during remarkable BSISO amplitude ≥ 1.5 SD for the ENSO neutral condition

Phase 3



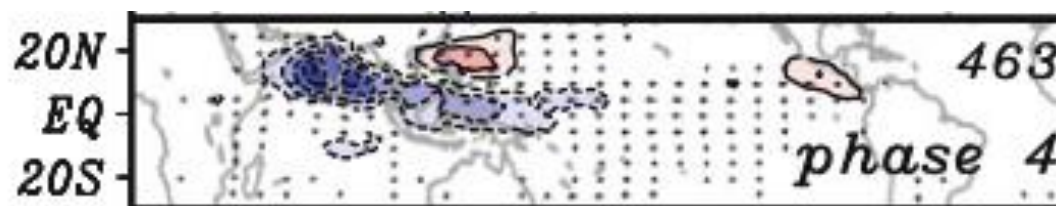
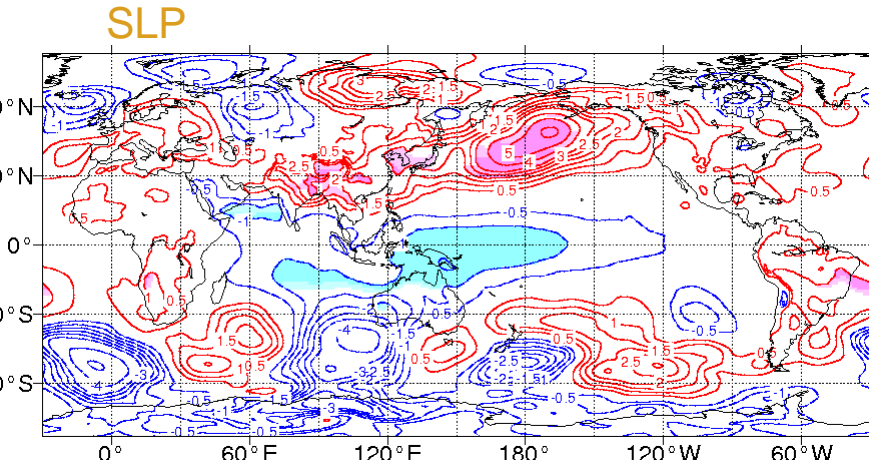
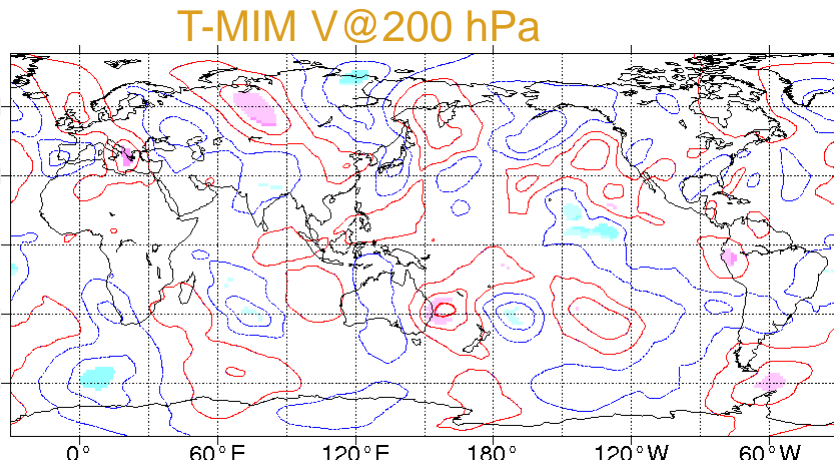
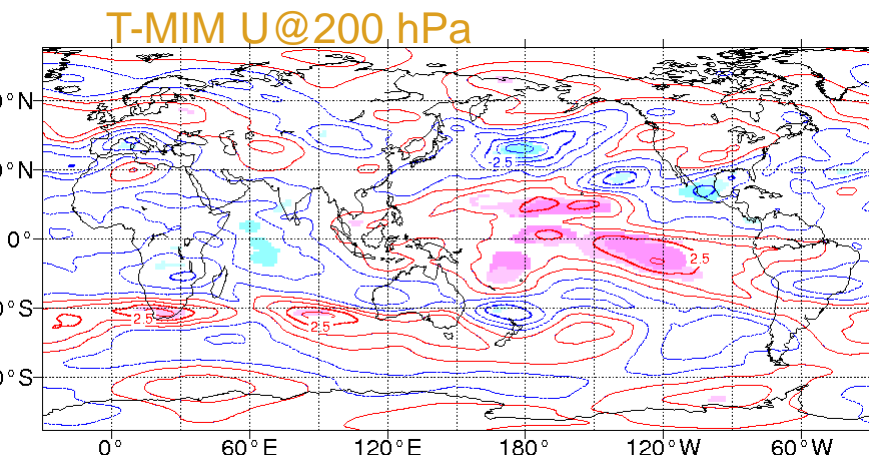
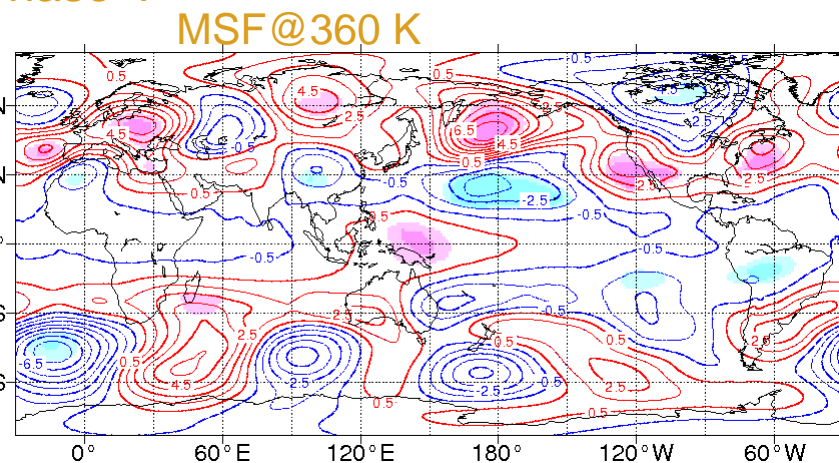
95 days
19 ESS
(Effective Sample Size)

Light (dark) shadings show statistical significance at 90 % (95 %) confidence levels.

Features of the global atmosphere during remarkable BSISO

amplitude ≥ 1.5 SD for the ENSO neutral condition

Phase 4



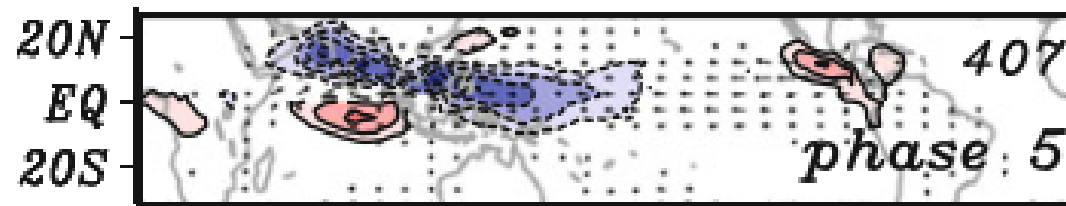
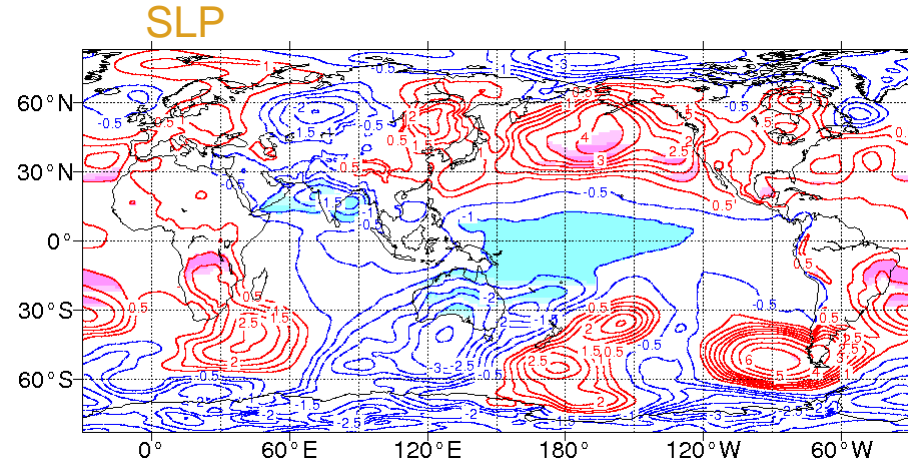
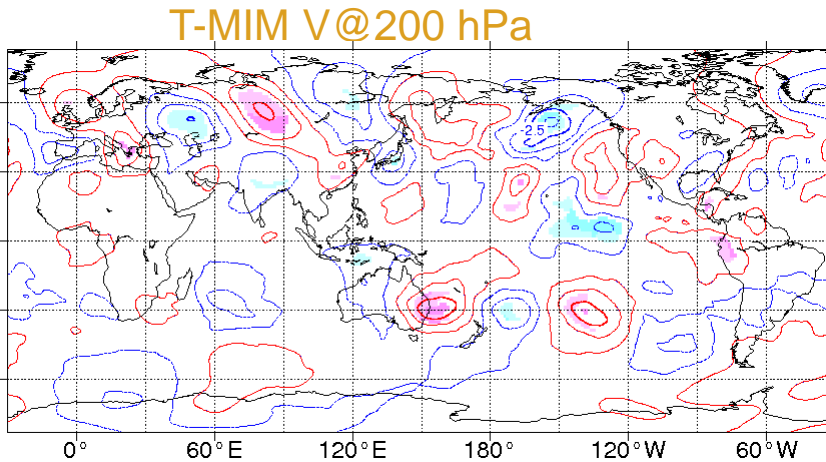
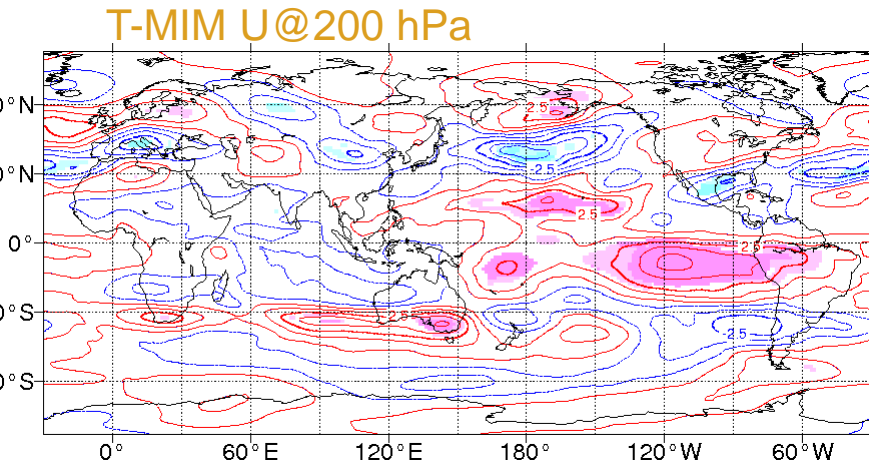
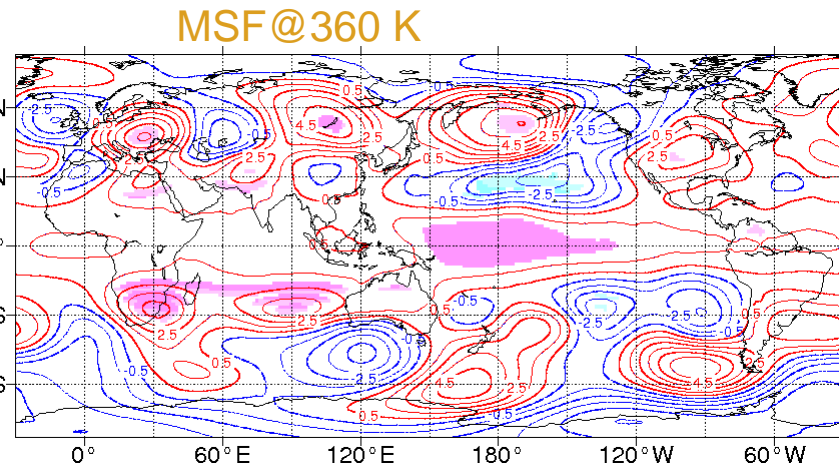
101 days
23 ESS
(Effective Sample Size)

Light (dark) shadings show statistical significance at 90 % (95 %) confidence levels.

Features of the global atmosphere during remarkable BSISO

amplitude ≥ 1.5 SD for the ENSO neutral condition

Phase 5

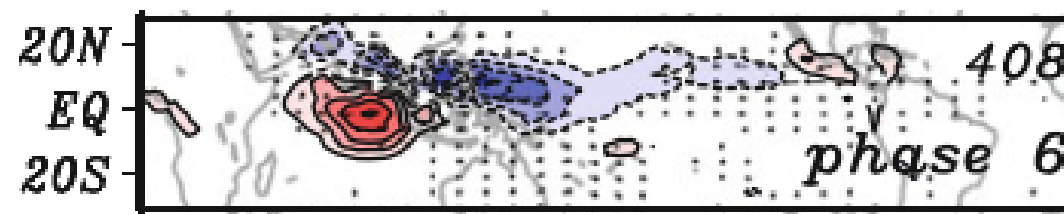
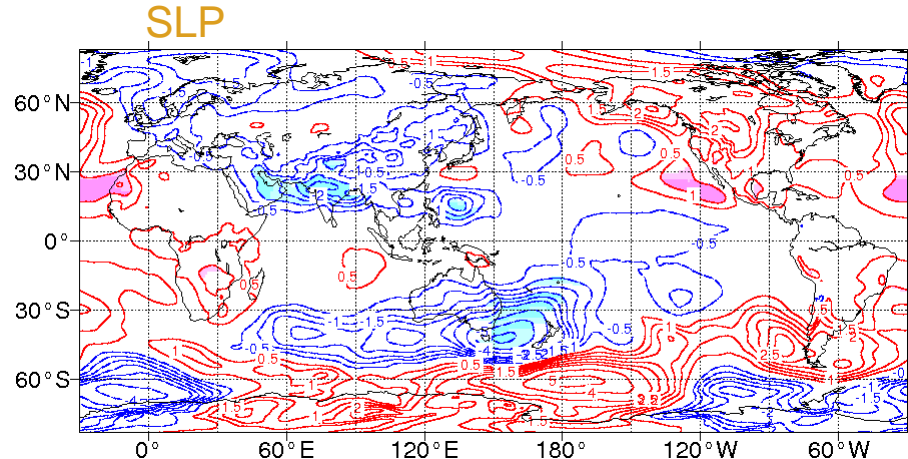
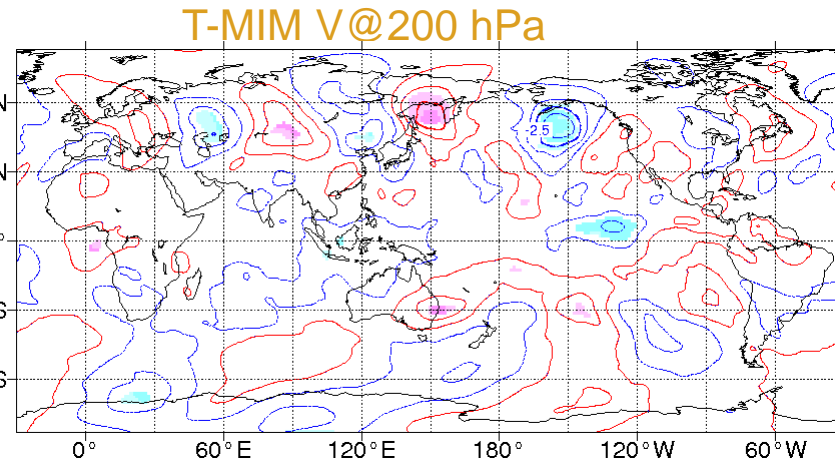
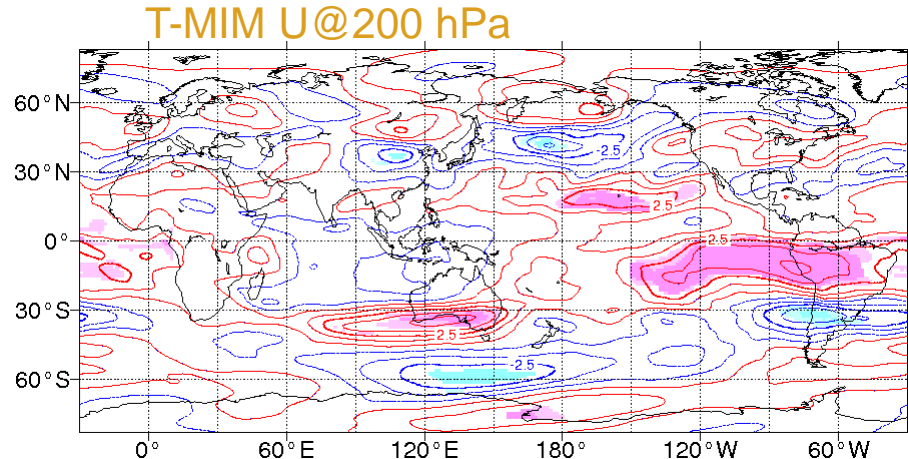
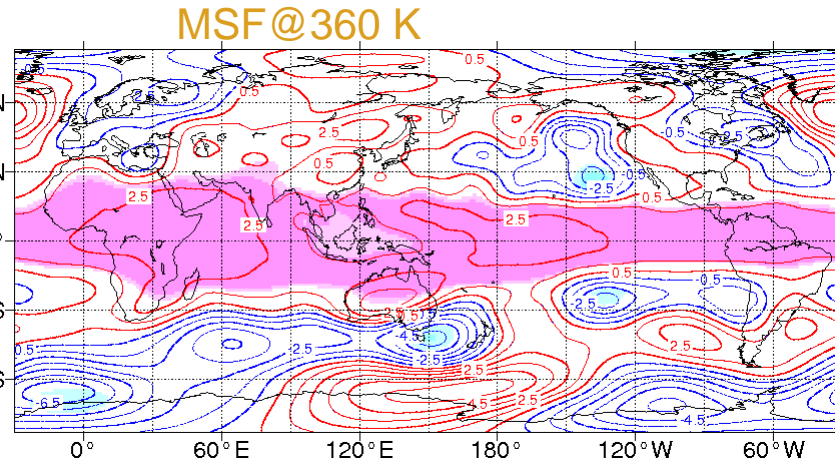


112 days
23 ESS
(Effective Sample Size)

Light (dark) shadings show statistical significance at 90 % (95 %) confidence levels.

Features of the global atmosphere during remarkable BSISO amplitude ≥ 1.5 SD for the ENSO neutral condition

Phase 6

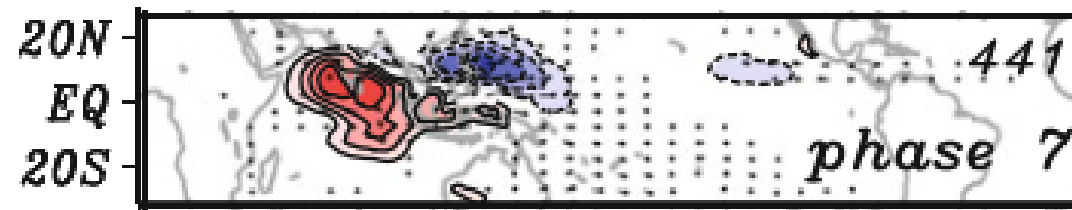
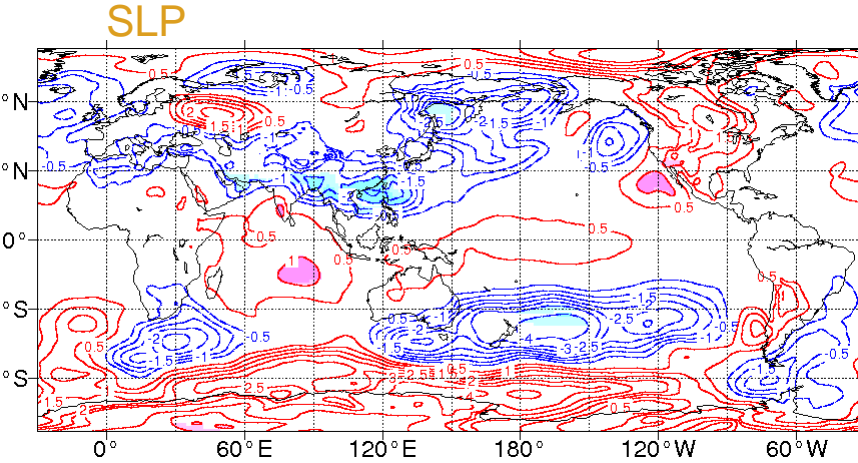
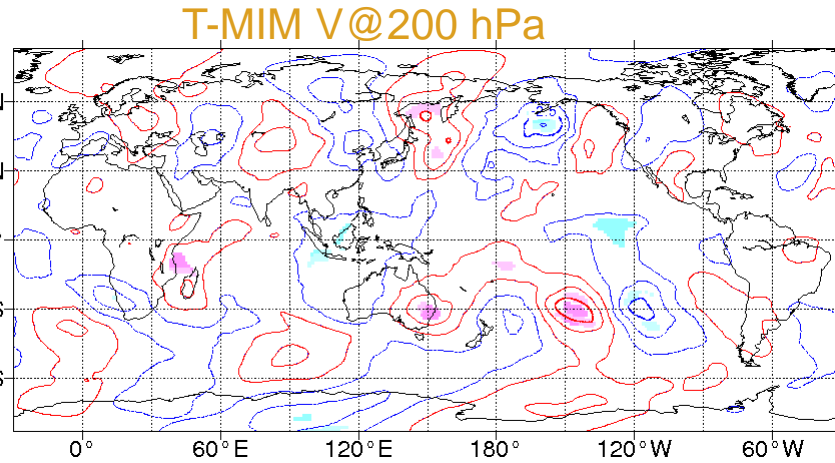
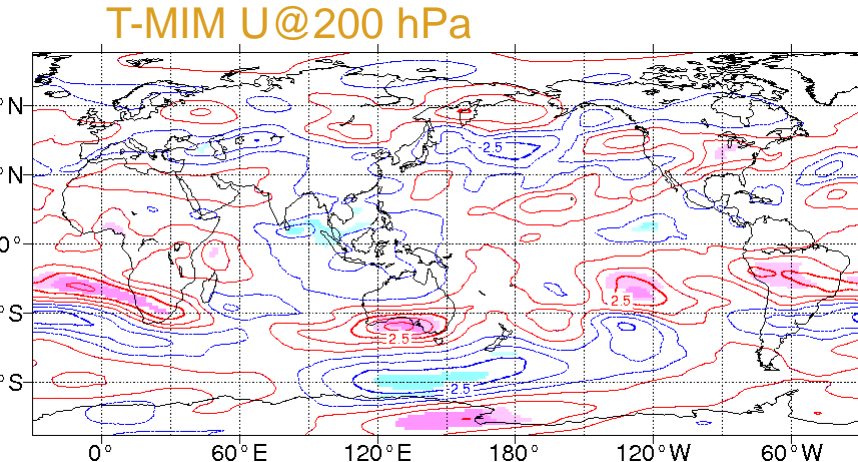
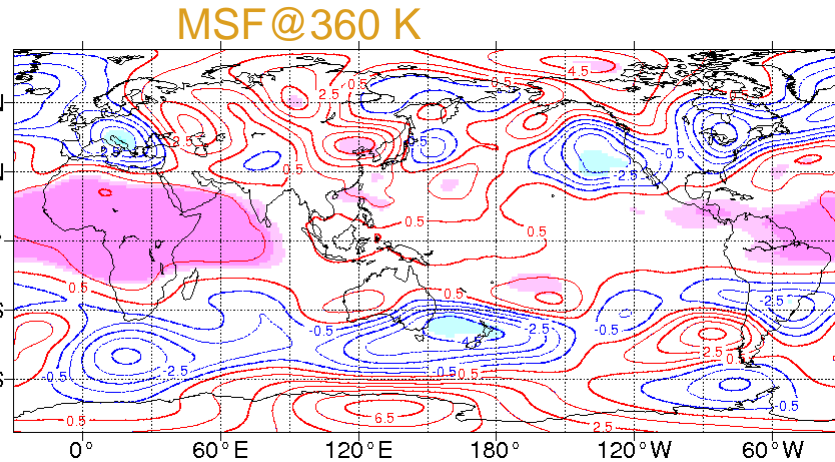


111 days
24 ESS
(Effective Sample Size)

Light (dark) shadings show statistical significance at 90 % (95 %) confidence levels.

Features of the global atmosphere during remarkable BSISO amplitude ≥ 1.5 SD for the ENSO neutral condition

Phase 7

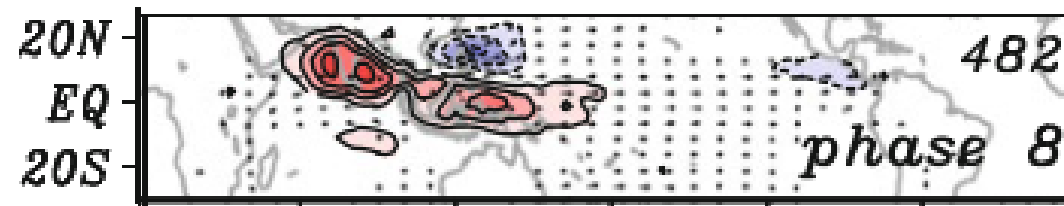
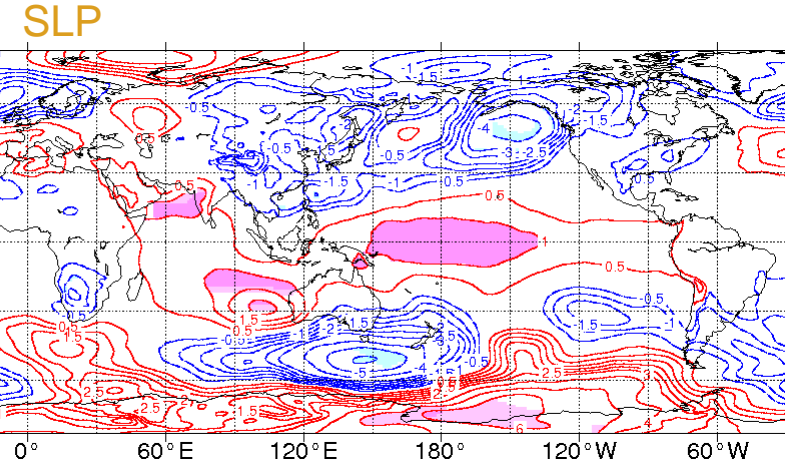
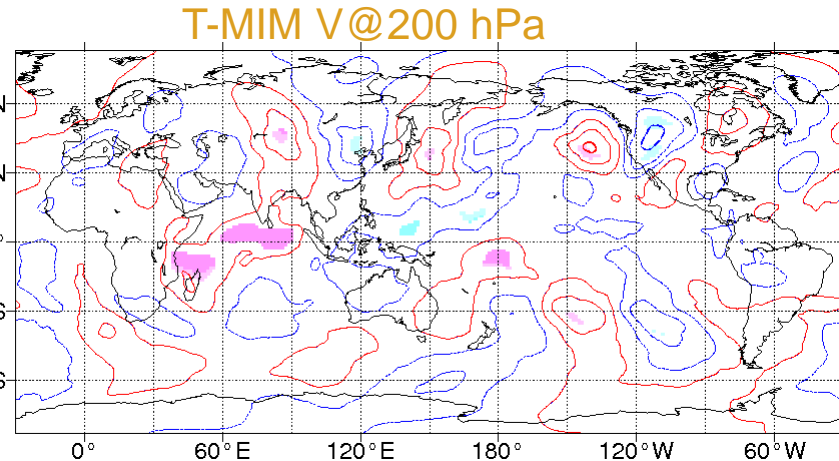
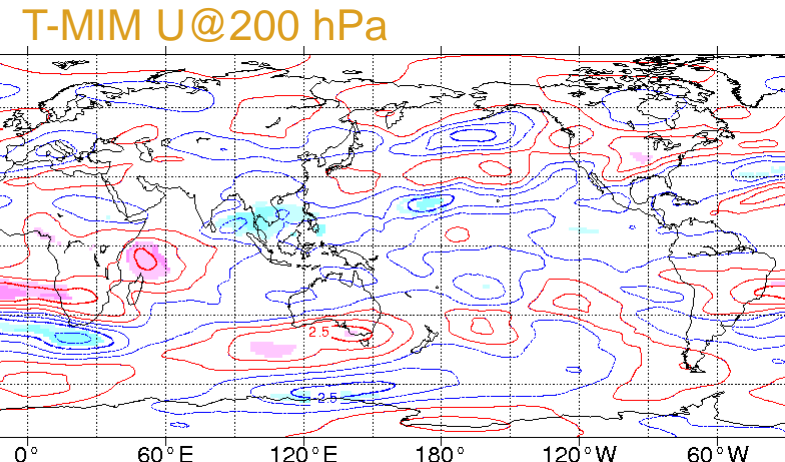
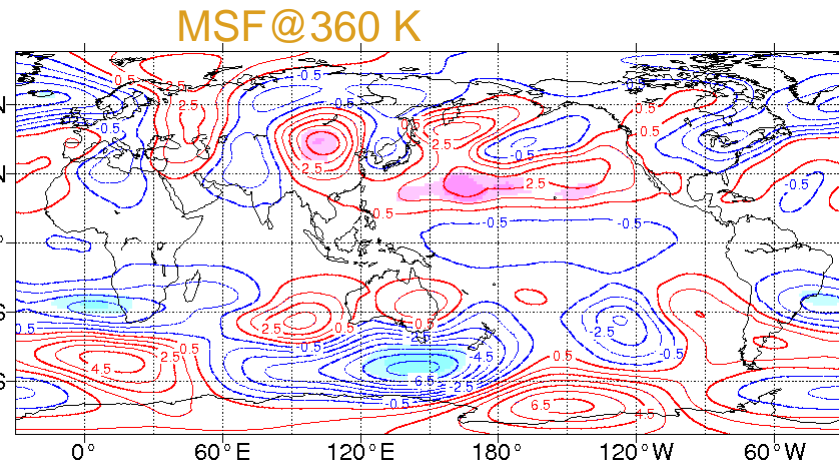


117 days
26 ESS
(Effective Sample Size)

Light (dark) shadings show statistical significance at 90 % (95 %) confidence levels.

Features of the global atmosphere during remarkable BSISO amplitude ≥ 1.5 SD for the ENSO neutral condition

Phase 8



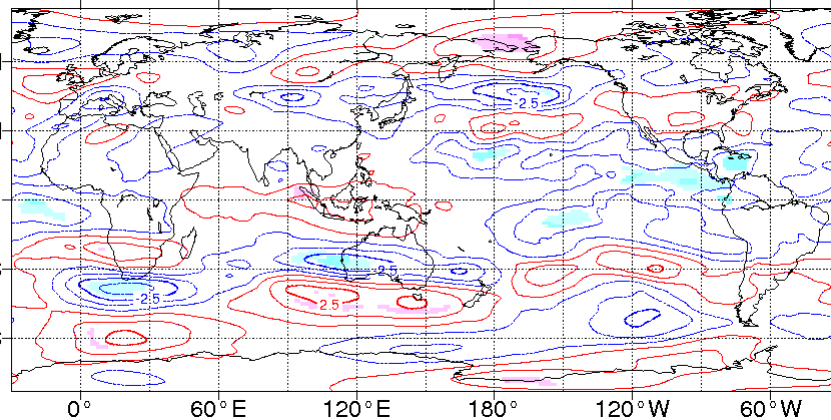
141 days
29 ESS
(Effective Sample Size)

Light (dark) shadings show statistical significance at 90 % (95 %) confidence levels.

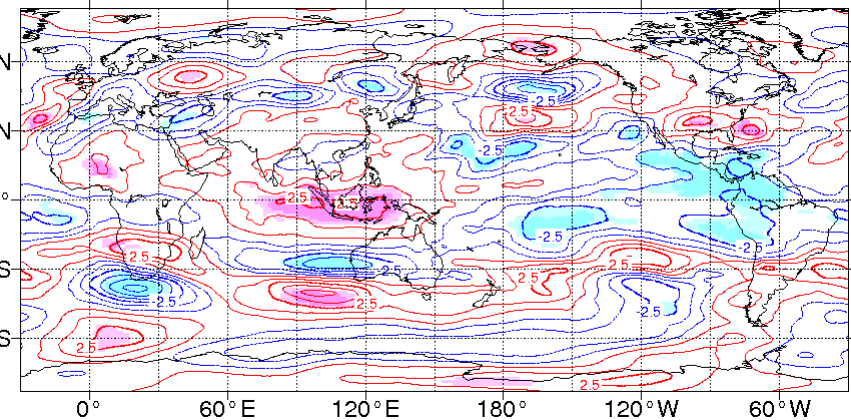
Comparison between amplitude ≥ 1.5 SD and amplitude ≥ 1.9 SD for the ENSO neutral condition

Phase 2

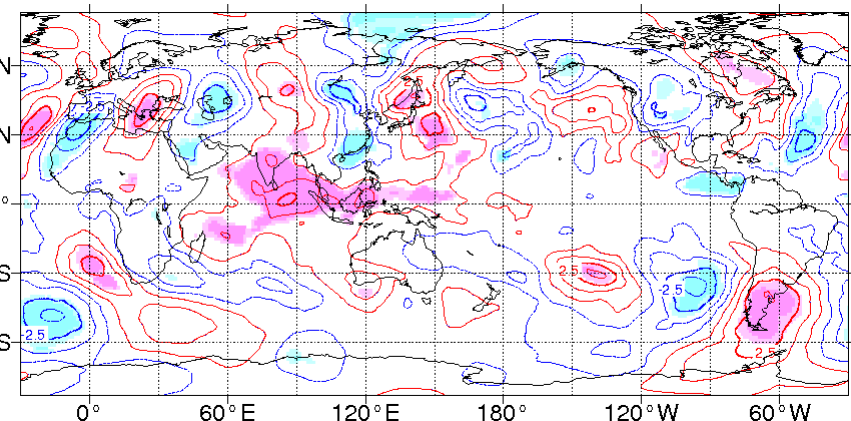
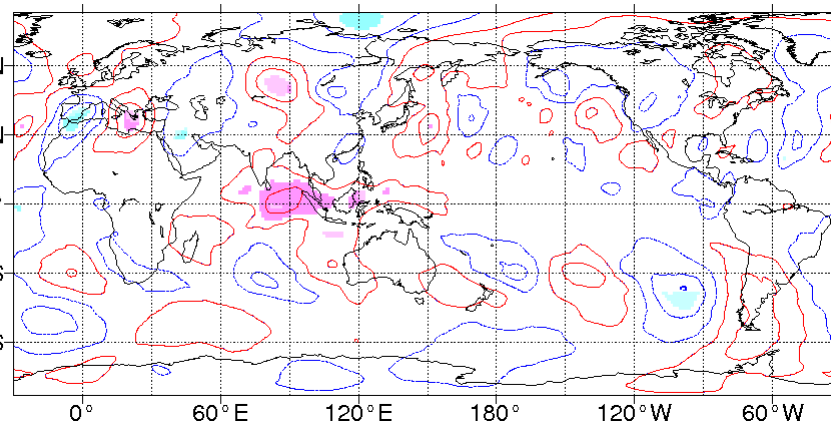
am amplitude ≥ 1.5 SD 96 days 23 ESS



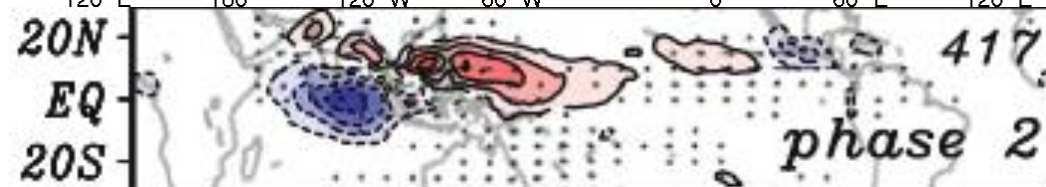
am amplitude ≥ 1.9 SD 46 days 11 ESS



T-MIM U@200 hPa



T-MIM V@200 hPa

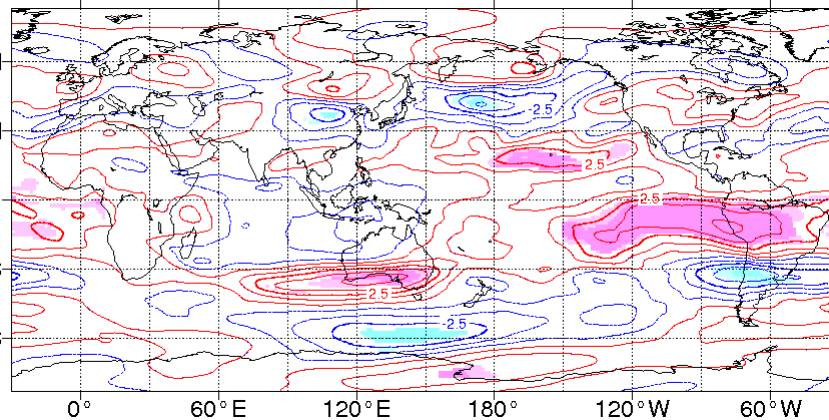


Light (dark) shadings show statistical significance at 90 % (95 %) confidence levels.

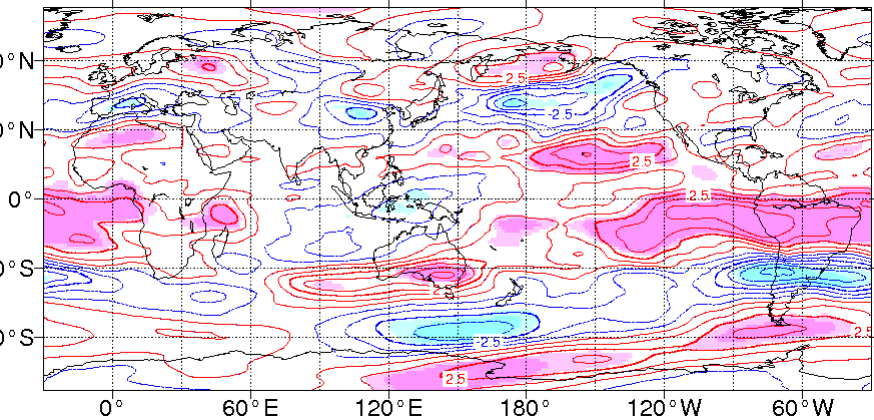
Comparison between amplitude ≥ 1.5 SD and amplitude ≥ 1.9 SD for the ENSO neutral condition

Phase 6

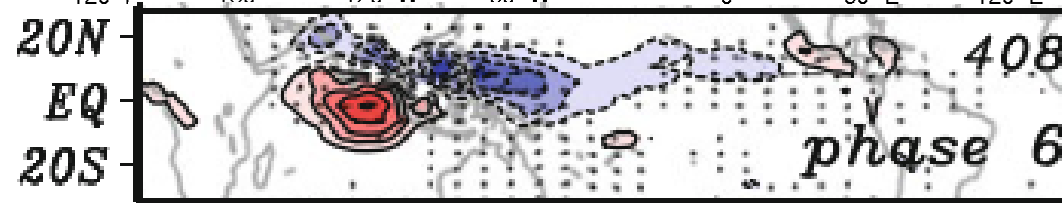
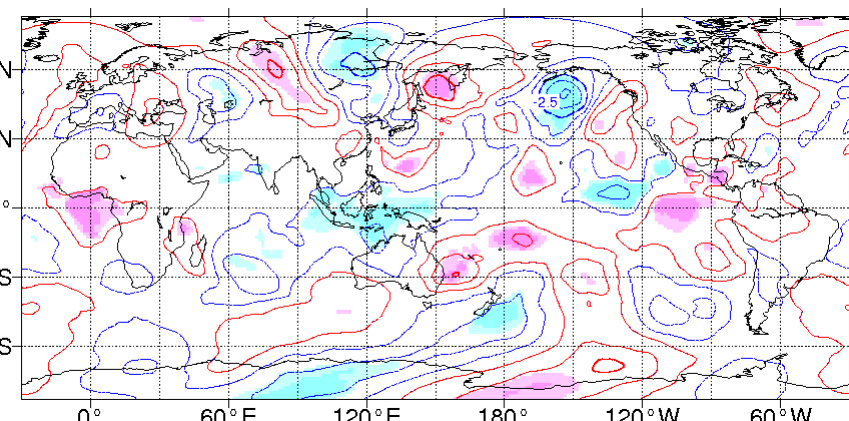
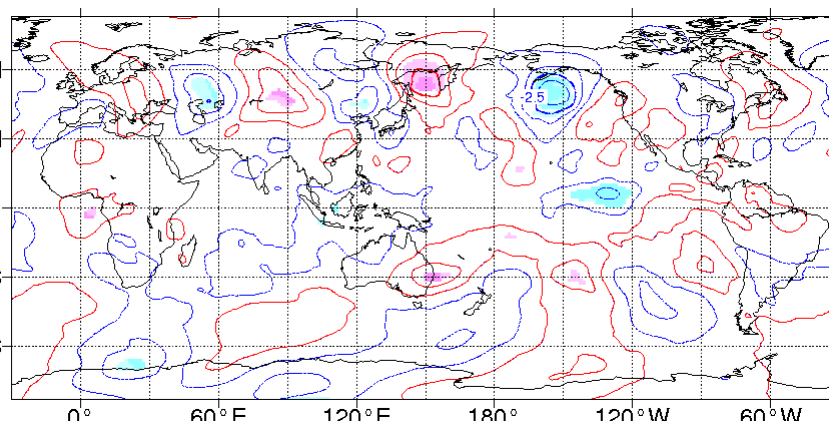
am amplitude ≥ 1.5 SD 111 days 24 ESS



am amplitude ≥ 1.9 SD 70 days 16 ESS



T-MIM V@200 hPa



95 days
19 ESS
(Effective Sample Size)

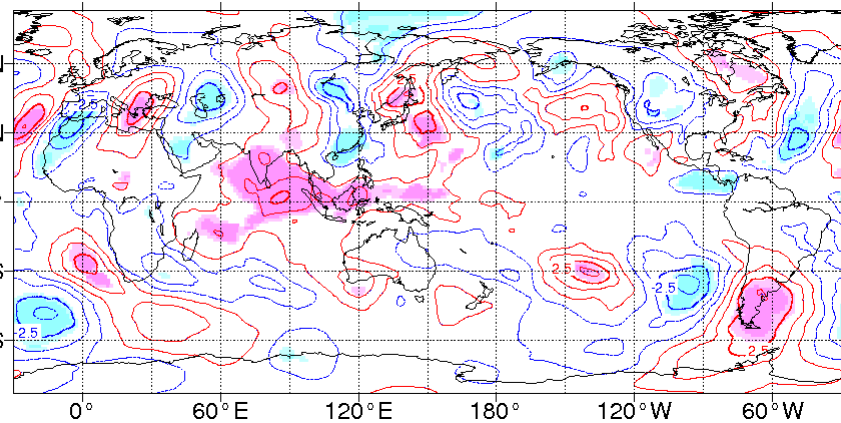
Light (dark) shadings show statistical significance at 90 % (95 %) confidence levels.

Comparison between Meridional wind and Forcing terms

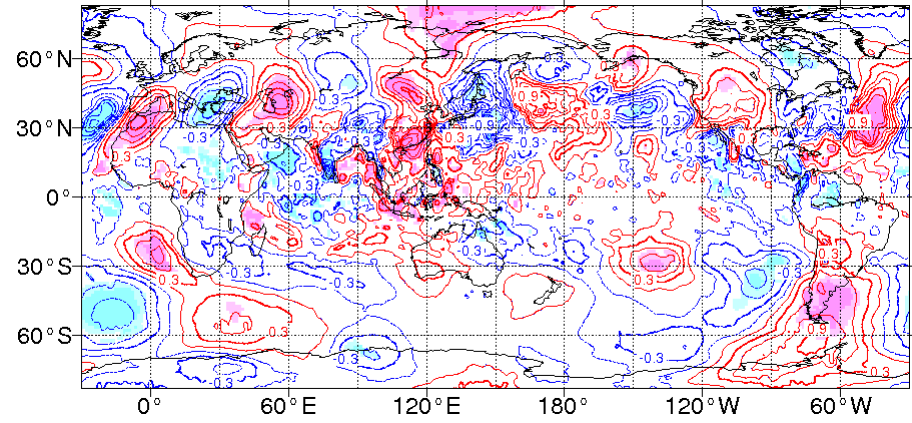
amplitude ≥ 1.9 SD for the ENSO neutral condition

Phase 2

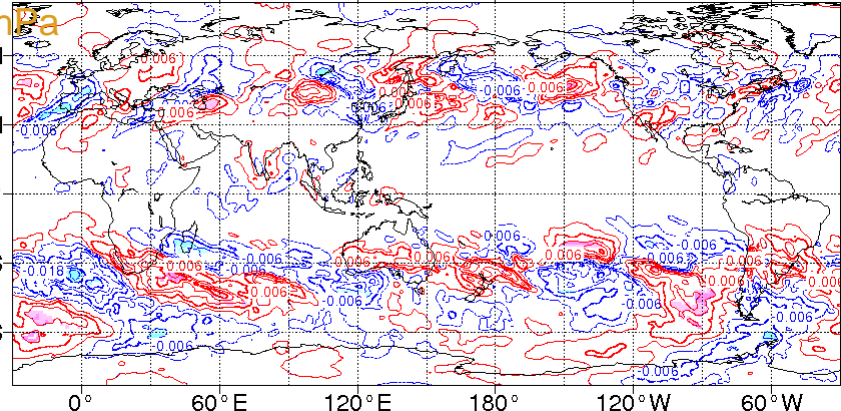
T-MIM V@200 hPa



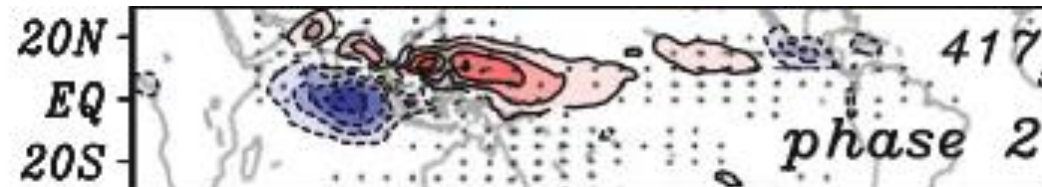
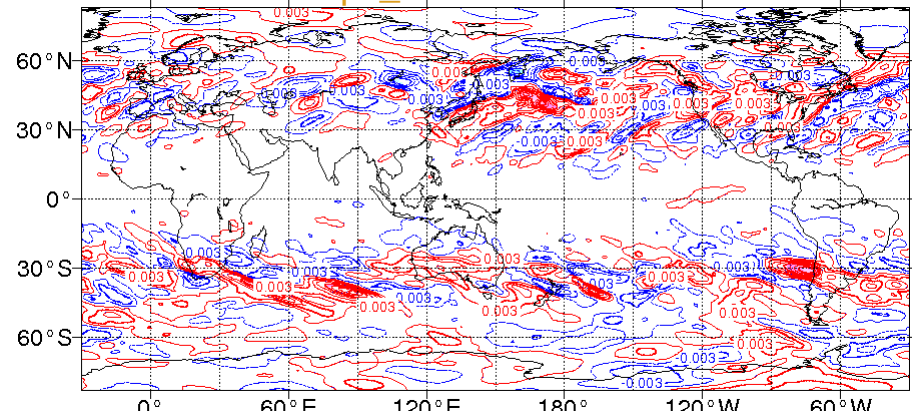
Div. of EPx_formz (all comp.)@200 hPa



Zonal advection of u by T-MIM zonal wind@200 hPa



Meridional div.of Epx_uv @200 hPa



46 days
11 ESS

Light (dark) shadings show statistical significance at 90 % (95 %) confidence levels.

まとめ

北半球夏季においてBSISO明瞭時には、

- 熱帯域では、対流活発位相の北進後(Phase5～7)に正の高度場偏差が明瞭。赤道域で対流活動活発時(Phase1～3)にはむしろ負の高度場偏差が明瞭。
- 北半球中緯度帯においても、有意な風東西成分偏差、定常波成分偏差が見られ、BSISOの振幅が強いほどこれらの偏差も強い傾向がある模様。

熱帯低気圧の発生頻度との関連？

基本場(風東西成分)の変動が波動の振幅に影響？

今後の課題、

- 等温位面のT-MIM要素、等温位面31日平均場などで合成図作成
- 強制項との比較の整理(EP-fluxの発散・収束、気圧傾度など)